

1 **Extracellular vesicles containing ACE2 efficiently prevent infection by SARS-**  
2 **CoV-2 Spike protein-containing virus**

3

4 Federico Coccozza<sup>1,2\*</sup>, Ester Piovesana<sup>1,2\*</sup>, Nathalie Névo<sup>1</sup>, Xavier Lahaye<sup>1</sup>, Julian  
5 Buchrieser<sup>3</sup>, Olivier Schwartz<sup>3</sup>, Nicolas Manel<sup>1</sup>, Mercedes Tkach<sup>1#</sup>, Clotilde Théry<sup>1#</sup>,  
6 Lorena Martin-Jaular<sup>1#</sup>

7

8 <sup>1</sup>INSERM U932, Institut Curie Centre de Recherche, PSL Research University, 75005 Paris,  
9 France.

10 <sup>2</sup> Université de Paris, 86 Bd St Germain, 75006 Paris, France.

11 <sup>3</sup> Virus and Immunity Unit, Institut Pasteur and CNRS UMR 3569, 75015 Paris, France.

12 \* : co-first authors (alphabetical order)

13 # : co-last and co-corresponding authors (alphabetical order): mercedes.tkach@curie.fr,  
14 clotilde.thery@curie.fr, lorena.martin-jaular@curie.fr

15

16 **ABSTRACT**

17 SARS-CoV-2 entry is mediated by binding of the spike protein (S) to the surface  
18 receptor ACE2 and subsequent priming by TMPRRS2 allowing membrane fusion.

19 Here, we produced extracellular vesicles (EVs) exposing ACE2 and demonstrate that  
20 ACE2-EVs are efficient decoys for SARS-CoV-2 S protein-containing lentivirus.

21 Reduction of infectivity positively correlates with the level of ACE2, is 500 to 1500  
22 times more efficient than with soluble ACE2 and further enhanced by the inclusion of  
23 TMPRSS2.

24

25 **MAIN**

26 SARS-CoV-2 is the causative agent of COVID-19 infection outbreak<sup>1</sup>. Viral entry into  
27 host cells is mediated by the interaction of the spike (S) protein on the surface of

28 SARS-CoV-2 with the surface receptor angiotensin-converting enzyme 2 (ACE2)<sup>2</sup>.  
29 After binding to ACE2, the S protein is cleaved by TMPRSS2 and becomes fusogenic  
30 thus allowing viral entry<sup>3</sup>. ACE2 is expressed at the surface of pneumocytes and  
31 intestinal epithelial cells which are potential target cells for infection<sup>4</sup>. Soluble  
32 recombinant ACE2 neutralizes SARS-CoV-2 by binding the S protein and has proven  
33 to reduce entry of SARS-CoV-2 in Vero-E6 cells and engineered human organoids<sup>5</sup>.  
34 ACE2 however is synthesized as a transmembrane protein, and we postulate that  
35 ACE2 could be present on the surface of extracellular vesicles (EVs) which could  
36 result in better efficacy as decoy to capture SARS-CoV-2.  
37 EVs are lipid bilayer enclosed structures containing transmembrane proteins,  
38 membrane associated proteins, cytosolic proteins and nucleic acids that are released  
39 into the environment by different cell types<sup>6</sup>. Since EVs have the same membrane  
40 orientation as the cells, they expose at their surface the extracellular domains of  
41 transmembrane proteins that can bind to short-distant or long-distant targets. By  
42 specifically binding to different proteins and protein-containing structures, EVs can  
43 act as a decoy for virus<sup>7</sup> and bacterial toxins<sup>8</sup>, thus having a potential role as  
44 therapeutic agents.  
45 In order to explore the hypothesis that EVs can be used as SARS-CoV-2 decoy  
46 agents we first assessed whether ACE2 can be present in EVs from two different  
47 sources: 1) cell lines derived from tissues expressing ACE2; and 2) 293FT cells  
48 overexpressing ACE2 and TMPRSS2. As cell lines naturally expressing ACE2 we  
49 used the human lung epithelial cell line Calu3 and the epithelial colorectal cell line  
50 Caco2 which are known targets for SARS-CoV2 infection<sup>3</sup>. Calu3 and Caco2 were  
51 cultured in medium without FBS for 24 hours and EVs were isolated from the cell  
52 conditioned medium (CCM) by size exclusion chromatography (SEC). This technique

53 allows the separation of EVs from soluble proteins (Figure 1A, Sup Figure 1A). We  
54 collected and analyzed EV-containing fractions, soluble protein-containing fractions  
55 and intermediate fractions containing a mixture of EVs and soluble components  
56 (Figure 1A, Sup Figure 1A). Particle quantification with nanoparticle tracking analysis  
57 (NTA) confirmed that the majority of particles released by Calu3 and Caco2 cells are  
58 isolated in EV-containing fractions (Figure 1B). Importantly, these EVs contain ACE2  
59 protein as well as known EV markers (CD63, CD81 and ADAM10) (Figure 1C).  
60 However, high amounts of soluble ACE2 are found in the intermediate and soluble  
61 fractions obtained from CCM of these cells. In addition, despite Caco2 and Calu3  
62 express TMPRSS2, this protease is not released in EVs or soluble fractions (Figure  
63 1C). To obtain EVs with high amounts of ACE2 and TMPRSS2 that can be used as  
64 a decoy agent, we transduced 293FT cells with lentivirus containing ACE2 alone  
65 (293FT-ACE2) or in combination with TMPRSS2 (293FT-ACE2-TMPRSS2). 293FT  
66 cells transduced with empty plasmids were used as a control (293FT-mock). The  
67 three 293FT cell lines were cultured in FBS-containing EV-depleted medium and EVs  
68 were isolated from CCM by SEC. We observed a high particle count in EVs fractions  
69 from 293FT cells (Figure 1B), coincident with the presence of CD63, CD81, Syntenin-  
70 1 and ADAM10 EV markers (Figure 1C). ACE2 is found enriched in EVs from ACE2-  
71 transduced 293FT cells when compared to soluble fractions. Importantly, EVs from  
72 293FT-mock and 293FT-ACE2 cells contain the cleaved form of TMPRSS2 whereas  
73 EVs from 293FT cells overexpressing TMPRSS2 also contain the full protein and its  
74 glycosylated form (Figure 1C)<sup>9</sup>. We detected also some particles in intermediate and  
75 soluble fractions from the three 293FT cell lines that are probably from the depleted  
76 medium and that do not contain EV markers by WB (Sup Figure 1B,1C).

77 We then analyzed the capacity of ACE2- and ACE2-TMPRSS2-containing EVs to  
78 reduce the infection of target cells by a lentivirus containing SARS-CoV-2-S protein.  
79 First, we determined the infectivity of the target cells Caco2, Calu3 and 293FT-ACE2  
80 by SARS-CoV-2-S-pseudotyped lentivirus and observed that all these cell lines are  
81 infected similarly in a concentration dependent manner (Figure 2A). To assess the  
82 ability of ACE2-containing EVs to decrease virus infectivity *in vitro*, we pre-incubated  
83 SARS-CoV-2-S-pseudotyped virus with EVs isolated from 293FT-mock (MOCK-EVs)  
84 or 293FT-ACE2 (ACE2-EVs) or 293FT-ACE2-TMPRSS2 cells (ACE2-TMPRSS2-  
85 EVs) prior to the infection of target cells (Figure 2B). Infection of 293FT-ACE2 cells in  
86 the presence of ACE2-EVs and ACE2-TMPRSS2-EVs was reduced while infection  
87 remained unaffected by MOCK-EVs (Figure 2C and quantification in 2D). Importantly,  
88 this inhibition was dependent on the dose of EVs. In addition to the effect of EVs on  
89 the infection of 293FT-ACE2, Caco2 infection was also reduced in the presence of  
90 ACE2-EVs and ACE2-TMPRSS2-EVs (Figure 2E). We then quantified by ELISA the  
91 amount of ACE2 released by these cell lines. We observed that 293FT-ACE2 cells  
92 release high levels of ACE2 that is associated to EVs while 293FT-ACE2-TMPRSS2  
93 cells release lower ACE2 levels that are equally distributed between EV and soluble  
94 fractions (Figure 2F). Strikingly, ACE2 in the soluble fractions from these latter cells  
95 was inefficient to inhibit SARS-CoV-2-S-pseudotyped virus infection as compared to  
96 the same amount of ACE2 associated to EVs (Figure 2G). Thus, considering the  
97 absolute amount of ACE2 present on EVs from these 293FT cell lines, we have  
98 observed that co-expression of the full length TMPRSS2 together with ACE2 on EVs  
99 results in a more efficient inhibition of SARS-CoV-2-S-pseudotyped viral infection  
100 (Figure 2H). Moreover, to achieve similar levels of inhibition of lentiviral infection as  
101 those observed with ACE2- or ACE2-TMPRSS2-EVs, 500 to 1500 times more of the

102 soluble recombinant human ACE2 had to be used (Figure 2H) in accordance to  
103 previous publications<sup>5</sup>. Altogether, these findings highlight the increased efficiency of  
104 EVs containing full-length ACE2 to inhibit SARS-CoV-2-S-pseudotyped viral entry  
105 when compared to the soluble protein alone.

106 Our data demonstrate that EVs containing ACE2, alone or in combination with  
107 TMPRRS2, block SARS-CoV-2 Spike-dependent infection in a much more efficient  
108 manner than soluble ACE2. Thus, ACE2-EVs represent a potential versatile  
109 therapeutic tool to block not only SARS-CoV2 infection but also other coronavirus  
110 infections that use the ACE2 receptor for host cell entry, as SARS-CoV<sup>10</sup> and NL63<sup>11</sup>.  
111 The use of engineered EVs as therapeutic agents has been proposed several years  
112 ago and is currently being explored in humans<sup>12</sup>, proving that a well-design EV  
113 therapeutics against COVID-19 is feasible.

114 Note: a speculative article discussing the idea that we demonstrate experimentally  
115 here was published while we were preparing this article, thus showing concomitant  
116 emergence of similar scientific ideas<sup>13</sup>.

## 117 **METHODS**

### 118 **Cells**

119 Human Caco-2 (HTB-37) and Calu-3 (HTB-55) were purchased from ATCC and  
120 maintained at 37°C in a humidified atmosphere with 5% CO<sub>2</sub>. Caco2 and Calu3 cells  
121 were cultured in DMEM (Sigma) supplemented with 10% FBS (Gibco), 100U/ml  
122 penicillin-streptomycin (Thermo Fisher Scientific) and non-essential aminoacids  
123 (Thermo Fisher Scientific). For Calu3 cells the medium was also supplemented with  
124 1mM sodium pyruvate (Thermo Fisher Scientific) and 10mM HEPES (Thermo Fisher  
125 Scientific). 293FT cells were cultured in DMEM medium (Sigma) supplemented with

126 10% FBS (Eurobio) and 100U/ml penicillin-streptomycin (Thermo Fisher Scientific).  
127 293FT-mock, 293FT-ACE2 and 293FT-ACE2-TMPRSS2 cells were generated by  
128 stable double transduction with pTRIP-SFFV-tagBFP-2A and pTRIP-SFFV-  
129 TagRFP657-2A, pTRIP-SFFV-tagBFP-2A-hACE2 and pTRIP-SFFV-TagRFP657-2A,  
130 or pTRIP-SFFV-tagBFP-2A-hACE2 and pTRIP-SFFV-TagRFP657-2A-TMPRSS2,  
131 respectively.

132

### 133 **Plasmids**

134 The plasmids psPAX2, CMV-VSVG, and pTRIP-SFFV-tagBFP-2A were previously  
135 described<sup>14</sup>. pTRIP-SFFV-TagRFP657-2A was generated by PCR from a synthetic  
136 gene coding for TagRFP657. pTRIP-SFFV-tagBFP-2A-hACE2 and pTRIP-SFFV-  
137 TagRFP657-2A-TMPRSS2 constructs were obtained by PCR from pLenti6-hACE2-  
138 BSD (hACE2 sequence from Addgene #1786 subcloned into pLenti6-BSD) and  
139 pCSDest-TMPRSS2 (Addgene #53887) respectively. A codon optimized version of  
140 the SARS-Cov-2 S gene (GenBank: QHD43416.1), was transferred into the pCMV  
141 backbone (GenBank: AJ318514), by replacing the VSV-G gene (pCMV-SARS-CoV-  
142 2-Spike)<sup>15</sup>. pCMV-SARS-CoV-2-S-H2 was obtained by PCR from pCMV-SARS-  
143 CoV-2-Spike in order to include the membrane-proximal region of the cytoplasmic  
144 domain of HIV-1 gp160 (NRVRQGYS, amino acid sequence)<sup>16</sup> after residue 1246 of  
145 the S protein<sup>17</sup>.

146

### 147 **Preparation of EV-depleted Medium**

148 EV-depleted medium was obtained by overnight ultracentrifugation of DMEM  
149 supplemented with 20% FBS at 100,000xg in a Type 45 Ti rotor (Beckman Coulter,  
150 K-factor 1042.2). After ultracentrifugation, EV-depleted supernatant was carefully

151 pipetted from the top and leaving 7 ml in the bottom. Supernatant was filtered  
152 through a 0.22  $\mu$ m bottle filter (Millipore) and additional DMEM and antibiotics were  
153 added to prepare complete medium (10% EV-depleted FBS medium).

154

#### 155 **EV isolation by Size-Exclusion Chromatography (SEC)**

156 239FT-mock, 293FT-ACE2 and 293FT-ACE2-TMPRSS2 cells were cultured in  
157 serum EV-depleted medium for 24h. Caco2 and Calu3 cells were cultured in FBS-  
158 free DMEM for 24h. Conditioned medium (CM) was harvested by pelleting cells at  
159 350xg for 5 min at 4°C three times. Supernatant was centrifuged at 2,000xg for 20  
160 min at 4°C to discard 2K pellet and concentrated on a Millipore Filter (MWCO = 10  
161 kDa, UCF701008) to obtain concentrated conditioned medium (CCM). Medium was  
162 concentrated from 12-41 ml for Caco2 and Calu3 and from 75 ml from 293FT cells to  
163 1 ml and overlaid on a 70nm qEV size-exclusion column (Izon, SP1). 0.5 ml fractions  
164 were collected and EVs were recovered in fractions 7 to 11 following manufacturer's  
165 instructions. We additionally collected intermediate fractions 12 to 16 and soluble  
166 factors in fractions 17 to 21, as we previously did to analyse AChE<sup>18</sup> Samples were  
167 additionally concentrated using 10kDa filter (Amicon, UCF801024) to reach a final  
168 volume of 100  $\mu$ l. Samples were stored at -80°C.

169

#### 170 **Nanoparticle Tracking Analysis (NTA)**

171 NTA was performed to analyze EV fractions, intermediate fractions and soluble  
172 fractions using ZetaView PMX-120 (Particle Metrix) with software version 8.04.02.  
173 The instrument was set a 22°C, sensitivity 77 and shutter of 70. Measurements were  
174 done using two different dilutions, at 11 different positions (3 cycles per position) and  
175 frame rate of 30 frames per second.

176

## 177 **Western Blotting (WB)**

178 Cell lysate was prepared using lysis buffer (50mM Tris, 150mM NaCl, 1% Triton,  
179 pH=8) supplemented with Phosphatase Inhibitor Cocktail (Sigma) at a concentration  
180 of  $4 \times 10^6$  cells in 100  $\mu$ L of buffer. After incubation for 20 min on ice, samples were  
181 centrifuged at  $18,500 \times g$  for 15 min. The pellet was discarded and the supernatant  
182 was kept for further analysis. EVs and the other SEC fractions were resuspended in  
183 1X Laemmli Sample Buffer (Biorad) and loaded in 4-15% Mini-Protean TGX Stain-  
184 Free gels (Biorad), under non-reducing conditions. Transferred membranes  
185 (Immuno-Blot PVDF Biorad) were developed using Clarity Western ECL substrate  
186 (Biorad) and the ChemiDoc Touch imager (Biorad). Antibodies for WB were anti-  
187 human: ACE2 (clone EPR4435, Abcam 108252), TMPRSS2 (clone EPR3681,  
188 Abcam 92323), ADAM10 (clone 163003, R&D Systems MAB1427), CD63 (clone  
189 H5C6, BD Bioscience 557305), Syntenin-1 (clone C2C3, Genetex GTX10847) and  
190 CD81 (clone 5A6, Santa Cruz sc-23692). Secondary antibodies included HRP-  
191 conjugated goat anti-rabbit IgG (H+L) (Jakson 111-035-144), HRP-conjugated goat  
192 anti-mouse IgG (H+L) (Jakson 111-035-146).

193

## 194 **Viral Production**

195 SARS-CoV-2-S-pseudotyped lentiviruses were produced by transient transfection of  
196 293FT cells in 150  $\text{cm}^2$  flasks with 5  $\mu$ g phCMV-SARS-Cov-2-S-H2, 13  $\mu$ g psPAX2  
197 and 20  $\mu$ g pTRIP-SFFV-eGFP-NLS and 114  $\mu$ l of TransIT-293 (Mirus Bio). One day  
198 after transfection, media was removed and fresh media was added. SARS-CoV-2-S-  
199 pseudotyped viruses supernatant was centrifuged at  $300 \times g$  for 10 min to remove  
200 dead cells, filtered with a 0.45  $\mu$ m filter (Millipore) and loaded on top of a 20%



201 sucrose gradient for concentration. Viral concentration was achieved by  
202 ultracentrifugation at 120,000xg for 1h 30 min in a SW32i rotor. The pellet containing  
203 concentrated SARS-CoV-2 S-pseudotyped virus was resuspended in 1 ml depleted  
204 DMEM and 100 µl aliquots were stored at -80°C.

205

## 206 **Infectivity Assay**

207 10,000-20,000 293FT-ACE2, Caco2 and Calu3 cells were seeded in a 96 well plate  
208 and after 6 h infected with SARS-CoV-2 S-pseudotyped virus in EV-depleted  
209 medium. Infection was performed in the absence or in the presence of different  
210 amount of EVs or human recombinant ACE2 (Abcam, 151852). Cells were then  
211 spinoculated at 1,200xg for 1h 30 min at 25°C. 48h after infection, cells were  
212 trypsinized, fixed and infection was measured by analyzing eGFP expression using a  
213 CytoflexLX cytometer. Data was analyzed using FlowJo software.

214

## 215 **ACE2 Enzyme-Linked Immunosorbent Assay (ELISA)**

216 Quantification of the amount of human ACE2 in the different EV and fractions was  
217 done using the human ACE2 ELISA kit (Abcam, ab235649) following manufacturer's  
218 instructions.

219

## 220 **REFERENCES**

- 221 1. Zhou, P. *et al.* A pneumonia outbreak associated with a new coronavirus of  
222 probable bat origin. *Nature* **579**, 270–273 (2020).
- 223 2. Walls, A. C. *et al.* Structure, Function, and Antigenicity of the SARS-CoV-2  
224 Spike Glycoprotein. *Cell* **181**, 281-292.e6 (2020).
- 225 3. Hoffmann, M. *et al.* SARS-CoV-2 Cell Entry Depends on ACE2 and TMPRSS2

- 226 and Is Blocked by a Clinically Proven Protease Inhibitor. *Cell* **181**, 271-280.e8  
227 (2020).
- 228 4. Ziegler, C. G. K. *et al.* SARS-CoV-2 Receptor ACE2 Is an Interferon-Stimulated  
229 Gene in Human Airway Epithelial Cells and Is Detected in Specific Cell  
230 Subsets across Tissues. *Cell* **181**, 1016-1035.e19 (2020).
- 231 5. Monteil, V. *et al.* Inhibition of SARS-CoV-2 Infections in Engineered Human  
232 Tissues Using Clinical-Grade Soluble Human ACE2. *Cell* **181**, 905-913.e7  
233 (2020).
- 234 6. Mathieu, M., Martin-Jaular, L., Lavieu, G. & Théry, C. Specificities of secretion  
235 and uptake of exosomes and other extracellular vesicles for cell-to-cell  
236 communication. *Nat. Cell Biol.* **21**, 9–17 (2019).
- 237 7. de Carvalho, J. V *et al.* Nef Neutralizes the Ability of Exosomes from CD4+ T  
238 Cells to Act as Decoys during HIV-1 Infection. *PLoS One* **9**, e113691 (2014).
- 239 8. Keller, M. D. *et al.* Decoy exosomes provide protection against bacterial toxins.  
240 *Nature* **579**, 260–264 (2020).
- 241 9. Afar, D. E. H. *et al.* Cancer Research. *Cancer Res.* **59**, 6015–6022 (2001).
- 242 10. Li, W. *et al.* Angiotensin-converting enzyme 2 is a functional receptor for the  
243 SARS coronavirus. *Nature* **426**, 450–454 (2003).
- 244 11. H, H. *et al.* Human Coronavirus NL63 Employs the Severe Acute Respiratory  
245 Syndrome Coronavirus Receptor for Cellular Entry. *Proc. Natl. Acad. Sci. U. S.*  
246 *A.* **102**, (2005).
- 247 12. Wiklander, O. P. B., Brennan, M. Á., Lötvall, J., Breakefield, X. O. &  
248 Andaloussi, S. EL. Advances in therapeutic applications of extracellular  
249 vesicles. *Sci. Transl. Med.* **11**, (2019).
- 250 13. Inal, J. M. Decoy ACE2-expressing extracellular vesicles that competitively

- 251 bind SARS-CoV-2 as a possible COVID-19 therapy. *Clin. Sci.* **134**, 1301–1304  
252 (2020).
- 253 14. Cerboni, S. *et al.* Intrinsic antiproliferative activity of the innate sensor STING in  
254 T lymphocytes. *J. Exp. Med.* **214**, 1769–1785 (2017).
- 255 15. Grzelak, L. *et al.* SARS-CoV-2 serological analysis of COVID-19 hospitalized  
256 patients, pauci-symptomatic individuals and blood donors. *medRxiv*  
257 2020.04.21.20068858 (2020). doi:10.1101/2020.04.21.20068858
- 258 16. F, M., E, K., J, S., A, B. & HG, G. Rescue of human immunodeficiency virus  
259 type 1 matrix protein mutants by envelope glycoproteins with short cytoplasmic  
260 domains. *J. Virol.* **69**, 3824–3830 (1995).
- 261 17. Moore, M. J. *et al.* Retroviruses Pseudotyped with the Severe Acute  
262 Respiratory Syndrome Coronavirus Spike Protein Efficiently Infect Cells  
263 Expressing Angiotensin-Converting Enzyme 2. *J. Virol.* **78**, 10628–10635  
264 (2004).
- 265 18. Liao, Z. *et al.* Acetylcholinesterase is not a generic marker of extracellular  
266 vesicles. *J. Extracell. Vesicles* **8**, (2019).

267

## 268 **ACKNOWLEDGEMENTS**

269 This work was supported by Institut Curie, INSERM, CNRS, grants H2020-MSCA-  
270 ITN (722148, TRAIN-EV), INCa (11548) and Fondation ARC (PGA1  
271 RF20180206962) to C Théry, LABEX DCBIOL (ANR-10-IDEX-0001-02 PSL\* and  
272 ANR-11-LABX-0043) to C. Théry and N. Manel, LABEX VRI (ANR-10-LABX-77),  
273 ANRS (France Re-cherche Nord & Sud Sida-hiv Hépatites; ECTZ36691,  
274 ECTZ71745), Sidaction (17-1-AAE-11097-2), ANR (ANR-19-CE15-0018-01, ANR-  
275 18-CE92-0022-01), DIM1HEALTH to N Manel.

276

## 277 **AUTHOR CONTRIBUTIONS**

278 FC, EP, NN, XL performed the experiments. FC, EP, MT, LMJ, CT analyzed the  
279 data. LMJ, CT, MT designed the experiments. EP, FC, MT, CT, LMJ wrote the  
280 paper. XL, NM and JB, OS designed plasmids, XL, NM generated cells  
281 overexpressing ACE2 and TMPRSS2 and developed the infection assay.

282

## 283 **FIGURE LEGENDS**

### 284 **Figure 1. Isolation and characterization of EVs containing ACE2 and TMPRSS2.**

285 (A) Scheme of EVs isolation and separation from soluble components by SEC. (B)  
286 NTA quantification of the particles produced by  $10^6$  cells contained in each fraction  
287 for different independent isolations. Error bars indicates SEM. (C) Western blot  
288 analysis of ACE2, TMPRSS2 and different EV markers in SEC fractions obtained  
289 from the five cell lines. Lysates from  $4 \times 10^5$  cells, EVs corresponding to  $0,5-1 \times 10^{10}$   
290 particles and intermediate and soluble fractions from the same number of producing  
291 cells ( $5-34 \times 10^6$  cells) as the EV (for Caco2 and Calu3) were loaded on the gels.  
292 Intermediate and soluble fractions from 1/10 and 1/20 producing cells ( $15-25 \times 10^6$   
293 cells), respectively, were loaded for 293FT-mock, 293FT-ACE2 and 293FT-ACE2-  
294 TMPRSS2.

295

### 296 **Figure 2. Inhibition of SARS-CoV-2-S-pseudotyped virus infection with ACE2**

297 **EVs.** (A) Infection of 293FT-ACE2, Caco2 and Calu3 cells with different dilutions of a  
298 SARS-CoV-2-S-pseudotyped lentivirus encoding for eGFP. The number of infected  
299 cells was calculated by multiplying the percentage of GFP-positive cells by the initial  
300 number of cells. (B) Scheme of the infectivity assay with different pre-treatments. (C)

301 Dot plots showing the percentage of infected 293FT-ACE2 cells obtained after  
302 incubation with viruses alone (1/10 dilution) or in combination with  $1 \times 10^{10}$  EV from  
303 the different 293FT cell lines. (D) Quantification of the percentage of infection of  
304 293FT-ACE2 cells after preincubation with EVs. eGFP+ cells were measured by  
305 FACS and normalized to infection with the virus alone (100%). Results from three  
306 independent experiments are shown. All replicates from each experiment are  
307 included. \*:  $p < 0.05$ ; \*\*:  $p < 0.01$ ; (Dunnett's test) (E) Caco2 infection in the presence of  
308 EV-ACE2 and EV-ACE2-TMPRSS2. (F) ACE2 quantification by ELISA in EV and  
309 Soluble fractions obtained from the three different 293FT cell lines. (G) Comparison  
310 of the effect on infection of EVs and soluble fractions from 293FT-ACE2-TMPRSS2.  
311 (H) Percentage of infected cells normalized to the amount of ACE2 present in EVs or  
312 as recombinant soluble form.

## FIGURE 1

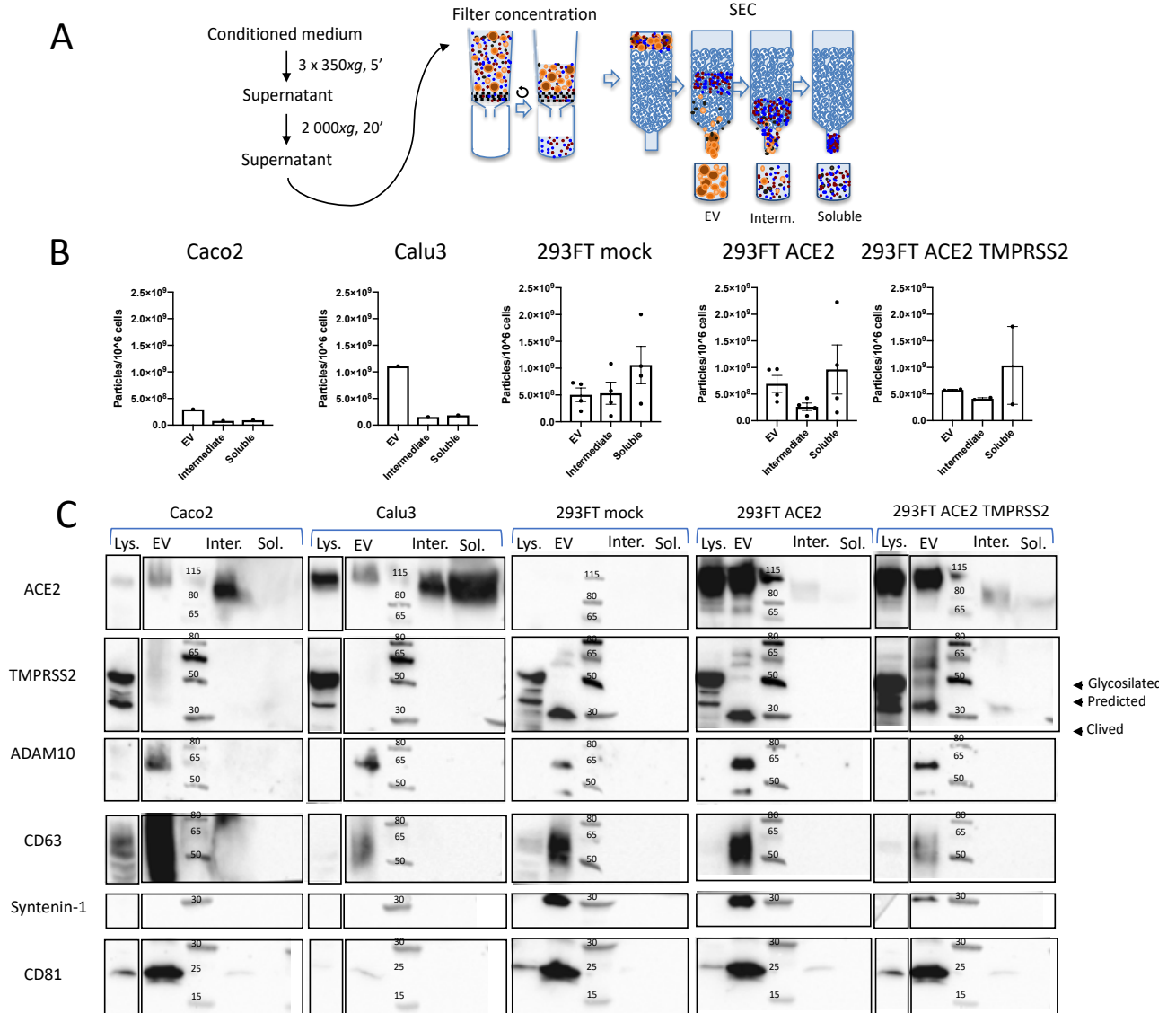
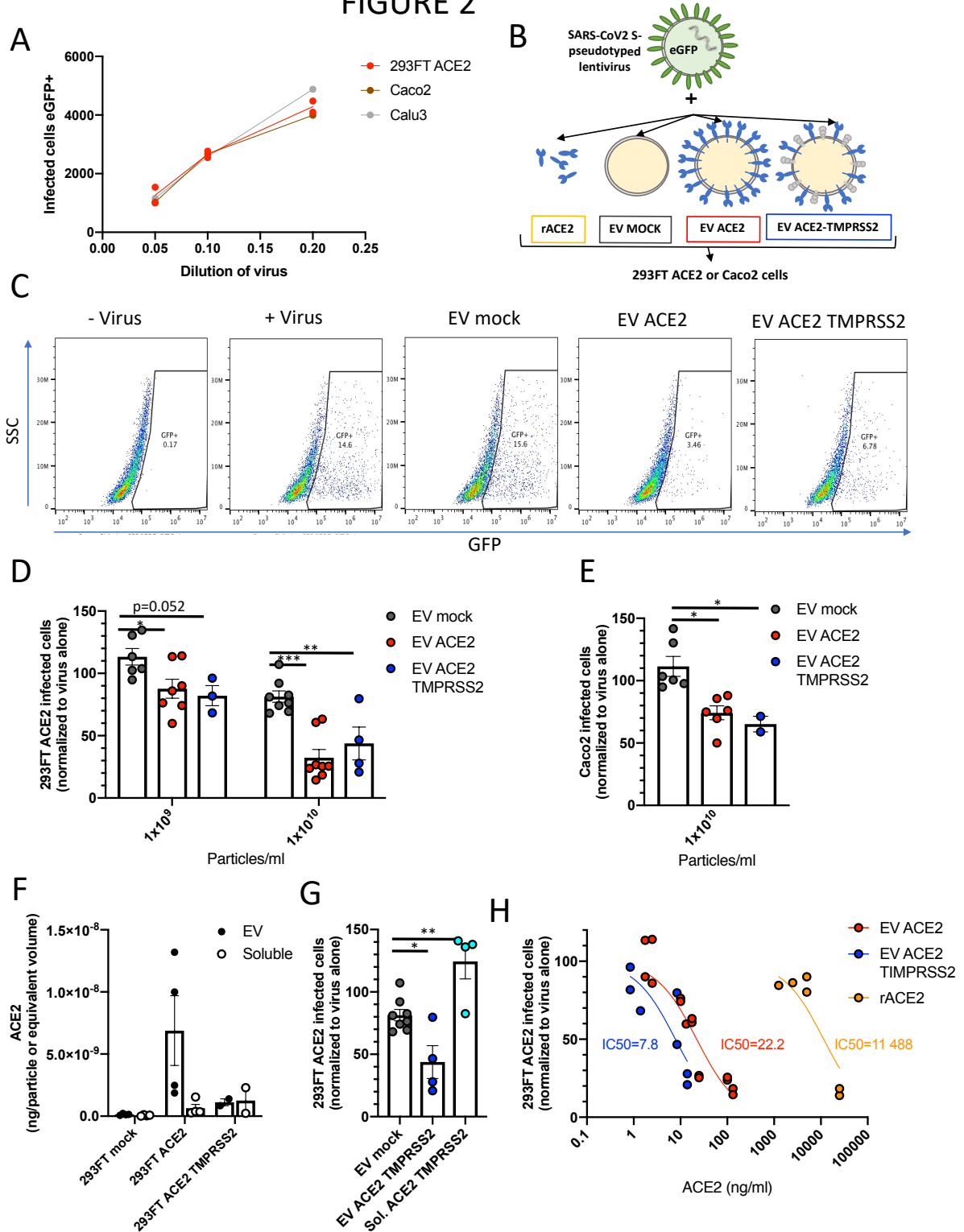
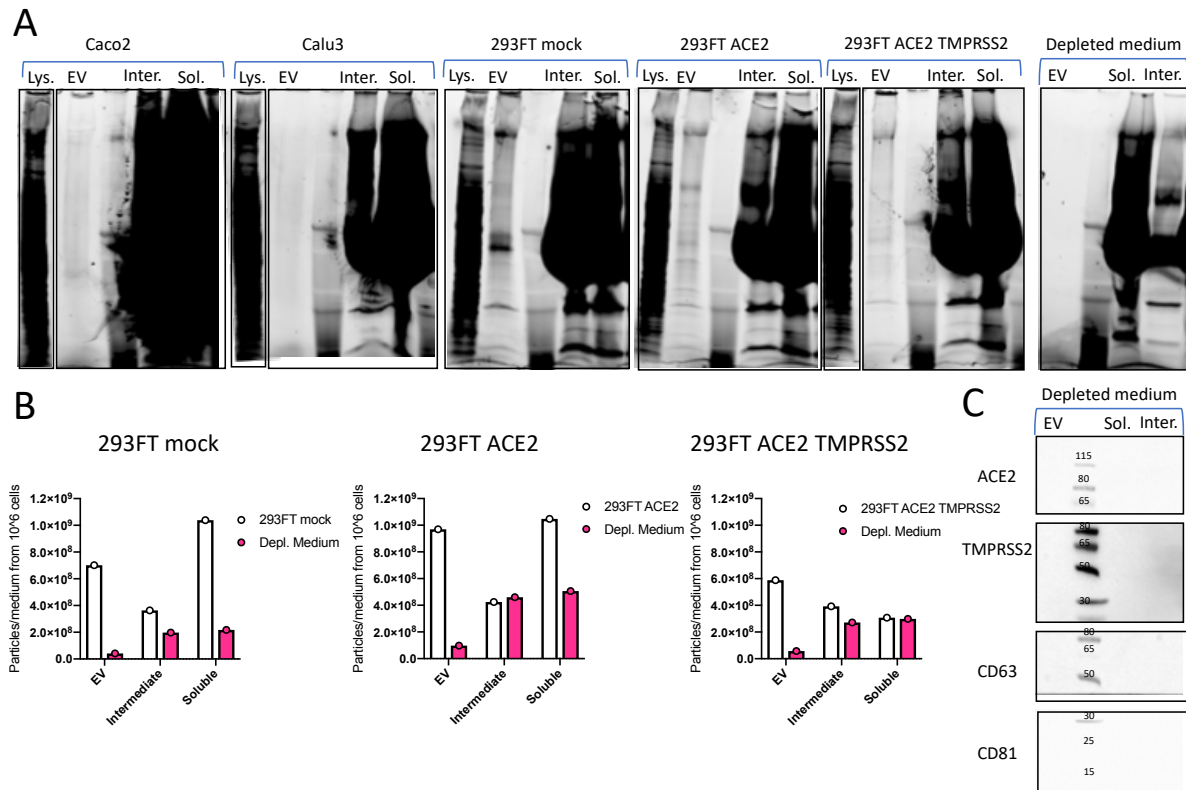


FIGURE 2



## Supplementary



**Supplementary Figure. Depleted medium particle contribution to the different fractions isolated by SEC.** (A) Protein stain-free images of gels used for WB in Figure 1C. (B) Number of particles counted in each fraction of 293FT-mock, 293FT-ACE2 and 293FT-ACE2-TMPRSS2 cell CCM, compared with non-conditioned depleted medium isolation performed in parallel. Numbers of particles are normalized to the volume of medium used for each purification. (C) Western blot analysis of non-conditioned depleted medium fractions isolated by SEC (material loaded on the WB was obtained from 15 ml initial volume of depleted medium for EV, 1,5 ml for intermediate and 0,75 ml for soluble).